Preparation of High-Modulus Nylon 6 Fibers by Vibrating Hot Drawing and Zone Annealing

TOSHIO KUNUGI, KIMITAKA CHIDA, AKIHIRO SUZUKI

Department of Applied Chemistry and Biotechnology, Faculty of Engineering, Yamanashi University, 4-3-11 Takeda, Kofu 400 Japan

Received 3 January 1997; revised 16 July 1997

ABSTRACT: To prepare high-modulus fibers, the vibrating hot-drawing and zone-annealing methods have been applied to nylon 6. The vibrating hot drawing was repeated two times, increasing the applied tension; further, the zone annealing was superposed on the vibrating hot-drawn fibers. The superstructure and mechanical properties of each step fiber were investigated. The vibration under a cooperation of heating and tension was very useful for increasing the draw ratio, birefringence, and orientation factor of the amorphous chains. Consequently, the obtained fiber indicated high moduli, namely, Young's modulus of 23 GPa and the dynamic storage modulus at room temperature of 25.3 GPa. © 1998 John Wiley & Sons, Inc. J Appl Polym Sci **67:** 1993–2000, 1998

Key words: nylon 6 fiber; vibrating hot-drawing method; high modulus; birefringence; orientation factor of amorphous chains

INTRODUCTION

Nylon 6 and 66 fibers are very important in the fabric industries, because they have excellent properties such as toughness and high melting point. To date, a variety of techniques have been proposed to improve the mechanical properties. Table I indicates the main methods[1–12] for nylon 6 with the chief researchers and the maximum values of modulus (E) and tensile strength (σ) in the order of the publications. There are interesting methods in the list, for example, the spinning of mixture of nylon 6 and lithium halide by Ciferris et al.[2] and Ward et al.,[4] the plasticization with ammonia or iodine by Porter et al.,[3,9] and the dry spinning of nylon 6 solution in formic acid/chloroform by Pennings et al.[8] However, the attained moduli are still low; even the maximum value in Table I is only 12.7% of the crystal modulus along molecular chains of 165 GPa.[13]

To overcome this situation, we had applied the vibrating hot-drawing and zone-annealing method to the nylon 6 fiber, which succeeded in a further improvement of the mechanical properties. The present article will describe the changes in superstructure and mechanical properties with the processing.

EXPERIMENTAL

Material

The original material was an as-spun nylon 6 fiber of 245 μm diameter, supplied by Toray Co. Ltd. The fiber has a crystallinity of 28.7%, a birefringence of 1.1×10^{-3}, and a melting point of 220.8°C.

Vibrating Hot Drawing

Figure 1 shows a scheme of apparatus used for the vibrating hot-drawing (VD) method.[14–16] The

Correspondence to: T. Kunugi.

Contract grant sponsor: Scientific Research of the Ministry of Education, Science, and Culture (Japan), and Eno Kagahu Shinko Zaidan.

Journal of Applied Polymer Science, Vol. 67, 1993–2000 (1998)
 CCC 0021-8995/98/121993-08

Table I Various Spinning, Drawing, and Annealing Methods for Nylon 6 Fibers and Films

Year	Method	Chief Researchers	E (GPa)	σ (GPa)	Ref.
1979	Zone drawing/zone annealing	Kunugi	8.3	1.0	1
1979	Spinning of mixture of nylon with LiCl/LiBr/drawing/annealing	Ciferris	14	—	2
1979	Plasticization with NH_3/coextrusion	Porter	13	0.6	3
1981	Spinning of mixture of nylon with LiCl/drawing/annealing	Ward	8	—	4
1981	Solution crystallization in 1,4-butandiol/solid-state coextrusion	Porter	6.7	—	5
1982	Zone drawing (one time)/Zone annealing (six times)	Kunugi	10.8	1.0	6
1983	Zone drawing (four times)/zone annealing (six times)/Heat setting	Kunugi	16.9	1.17	7
1985	Dissolution in formic acid/chloroform/dry spinning/hot drawing	Pennings	19	1.0	8
1986	Plasticization with iodine/drawing at 55°C/removal of iodine	Porter	6	—	9
1986	Gellation with benzyl alcohol/partially dried film/coextrusion	Porter	5.6	—	10
1993	Repeated heating and cooling cycles under sinusoidal deformation	Kunugi	21	—	11
1993	High-temperature zone drawing/heat treatment under high tension	Kunugi	21.1*	1.11	12

apparatus consists of an amplifier, a vibrator equipped with an accelerometer, and an electric furnace. One end of the fiber was fixed at the vibrator head, and the other end was attached to a dead weight so that a suitable tension occurs. The fiber was heated in the electric furnace at a desired temperature. The vibration frequency (f) can be selected in the range from 2 to 20,000 Hz. Also, the optimum amplitude was selected so that the draw ratio is as high as possible. The conditions for the VD are the drawing temperature, applied tension, vibration frequency, and amplitude. These factors were determined so that the tensile modulus becomes higher. The VD was applied two times to the same fiber increasing the tension. After a number of preliminary experiments, the conditions shown in Table II were decided. The treatment time was 10 min for each step.

Zone Annealing

Figure 2 shows the apparatus used for the zone-annealing method (ZA).[1,6,7,17] One end of the fiber was fixed at the flame and the other end was attached to a dead weight. The narrow part of the fiber was heated by a zone heater. The zone heater is set on the shaft of a lineard motor, and can be moved along the fiber axis at a suitable speed. The conditions for the ZA are the heater temperature, applied tension, and heater speed. The optimum conditions are also shown in Table II. The heater speed was 50 mm/min.

Measurements

The birefringence (Δ_t) was measured with a polarizing microscope equipped with a Berec compensator. As additional compensators, X-Z planes of various thicknesses cut from a single crystal of quartz were used on the measurements. The orientation factor of crystallites (f_c) was evaluated by means of eq. (1).

$$f_c = 1 - (3/2)\langle \sin^2\alpha \rangle \quad (1)$$

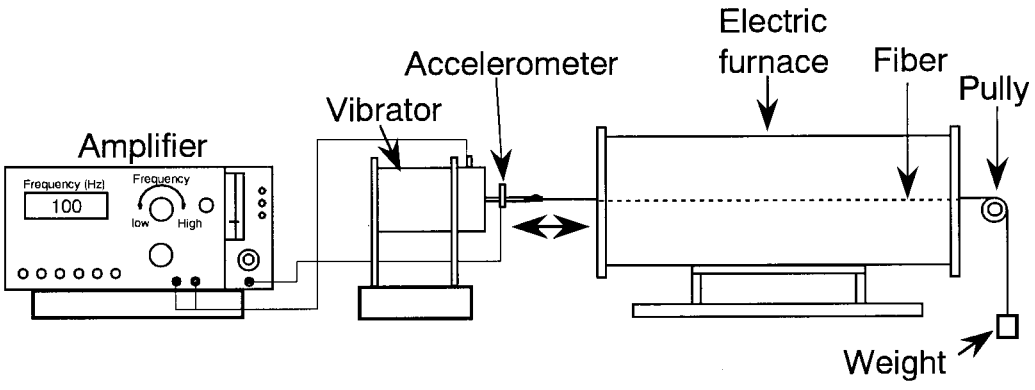

Figure 1 Scheme of apparatus used for the vibrating hot-drawing method.

Table II Conditions for Vibrating Hot Drawing

Step	Drawing Temperature (°C)	Applied Tension (kg/mm^2)	Frequency (Hz)	Amplitude (μm)
VD-1	190	2.8	10	400
VD-2	190	23.0	10	400
ZA	200	28.4	—	—

where α is the angle between fiber axis and the crystallographic b-axis, and $\langle \sin^2\alpha \rangle$ can be calculated from eq. (2), which was proposed by Kunugi et al.[18]

$$\langle \sin^2\alpha \rangle = \langle \sin^2\beta_{h01} \rangle + \langle \sin^2\beta_{002} \rangle \quad (2)$$

where the $(h01)$ plane is an imaginary plane that is perpendicular to the (002) plane. The β_{002}, β_{200}, and β_{h01} represent the angles between the normal vector of each plane and the equator, respectively.

The $\langle \sin^2\beta_{h01} \rangle$ can be calculated from the following equation.

$$\langle \sin^2\beta_{h01} \rangle = (\langle \sin^2\beta_{200} \rangle - \sin^2 22.5° \cdot \langle \sin^2\beta_{002} \rangle)/\cos^2 22.5° \quad (3)$$

where $\langle \sin^2\beta_{200} \rangle$ or $\langle \sin^2\beta_{002} \rangle$ was graphically determined from the azimuthal intensity distribution of X-ray diffraction for the (200) or (002) plane.

The orientation factor of amorphous chains (f_a) was calculated by substituting the f_c, crystallinity (X), and intrinsic birefringences of the crystallites and amorphous chains (Δ_c and Δ_a) into the following equation.

$$f_a = (\Delta t - X \cdot f_c \cdot \Delta_c)/(1 - X)\Delta_a \quad (4)$$

where Δ_c and Δ_a values of 0.078 and 0.069 were used in the above calculation, respectively, which was proposed by Kunugi et al.[19]

The density (d) was measured at 25°C by a flotation method using toluene–carbon tetrachloride mixtures. The X was calculated by the usual method using a crystal density of 1.230 g/cm^3 and an amorphous density of 1.084 g/cm^3.

The crystallites sizes (D_{200}, D_{002}, and D_{0140}) were determined by means of Scherrer's eq. (5) from the half-width of the diffraction peaks (β) for each plane.

$$D_{hkl} = k \cdot \lambda/(\beta \cdot \cos\theta) \quad (5)$$

where k, λ, and θ are the constant, wave length, and the Bragg angle, respectively. The differential scanning calorimeter (DSC) curves and the heat of fusion (ΔH_f) were obtained at a heating rate of 10°C/min with DSC 8230C, TAS-200 type (Rigaku Co., Ltd.).

The dynamic viscoelastic properties (E', E'', and tan δ) were measured at 110 Hz, at a heating rate of 1.5°C/min in a stream of nitrogen gas with a dynamic viscoelastometer, Vibron RHEO-200 type, Model DDV-II-C (Orientec Co. Ltd.). The tensile properties (Young's modulus, tensile strength, and elongation at break) were measured at 22°C and RH ca. 60% at a strain rate of 10%/min with a tensile tester, Tensilon UTM-II-20 type (Orientec Co. Ltd.).

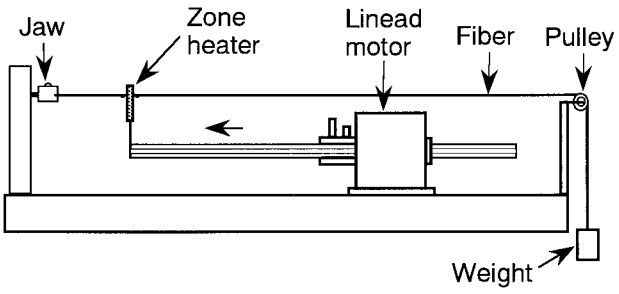

Figure 2 Scheme of apparatus used for the zone-annealing method.

Table III Draw Ratio (DR), Birefringence (Δ_t), Orientation Factors of Crystallites, and Amorphous Chains (f_c and f_a) for Each Step Fiber

Step	DR	Δ_t ($\times 10^3$)	f_c	f_a
Original	1.0	1.1	—	—
VD-1	5.5	63.5	0.98	0.69
VD-2	5.7	66.3	0.99	0.79
ZA	6.0	67.1	0.99	0.80

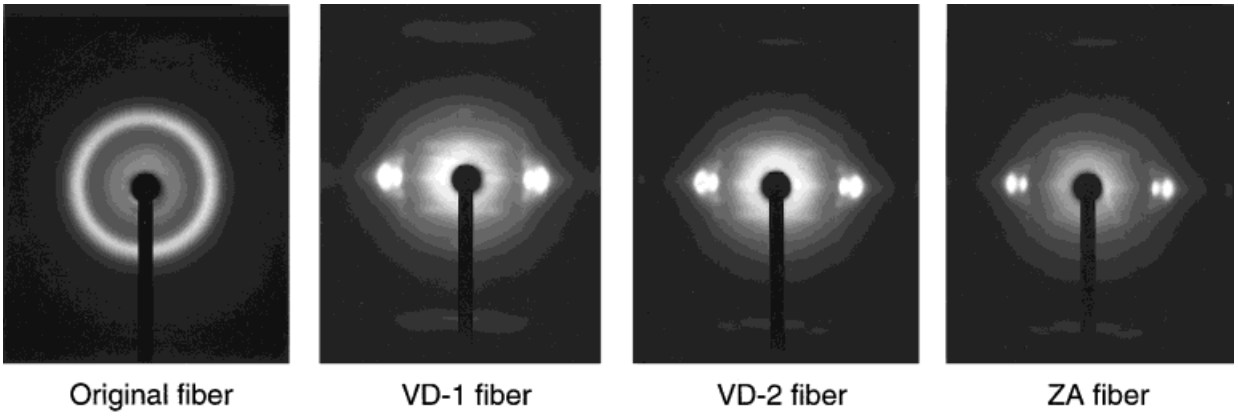

Figure 3 Wide-angle X-ray diffraction photographs for the original, VD-1, VD-2, and ZA fibers.

RESULTS AND DISCUSSION

Drawing of Nylon 6 Fibers

It is often said that the hydrogen bonds and crystallites inhibit a high drawability in the case of nylon fibers.

So far, we have reported that the hydrogen bonds in amorphous region are weakened or broken above 70–120°C. This became apparent from the results of measurements on thermal shrinkage,[20] stress relaxation,[21] thermal stress,[20] and dynamic viscoelasticity[22–24] for cold-drawn nylon 6 fibers. In all measurements, two-step temperature dependence starting at room temperature and around 90°C were observed. We considered that the first step is attributed to glass transition and the second step takes place by breakdown of inter- or intramolecular hydrogen bonds in amorphous region. The second step variations are very sensitive to the differences in superstructure caused by cold drawing and heat treatment.

For example, the second thermal shrinkage[20] starts at 80°C for the fibers cold drawn, but 100°C for the fibers cold drawn after heat treatment. In the stress relaxations,[21] the relation between the logarithm of shift factor ($\log a_T$) and the reciprocal of temperature ($1/T$) was indicated by two straight lines intersecting at one point. The break point implies the change in mobility of molecular segments having different apparent activation energies at above and below the point. The hydrogen bonds are broken down at the temperature near the point. The temperatures of the break point were 371 K (98°C) for the threefold cold-drawn fiber and 350 K (77°C) for the fourfold cold-drawn fiber. In the case of the fourfold cold-drawn fiber, for example, the apparent activation energies were 33 kcal/mol in the higher temperature region and 49 kcal/mol in the lower temperature region. Further, the thermal stress curve for a fiber cold drawn up to twofold after heat treatment indicated two peaks centered at 60 and 120°C. Finally, the dynamic viscoelasticity indicates α dispersion peak, which is assigned to the micro-Brownian motion of large molecular segments due to breakdown of hydrogen bonds in the amorphous regions. The dispersion peak occurs in the range from 70 to 130°C in tan δ–temperature curves.

From the above various results, it is clear that the interference from hydrogen bonds on drawing can be prevented, if the nylon 6 fibers are drawn at a temperature above 150°C. Furthermore, the tension and vibration during drawing have effects to reduce a necessary drawing temperature.

On the other hand, the crystallites also inhibit the high drawability of fibers by acting as aggregation points of molecular chains. In the case of nylon 6, there are two kinds of crystallites. One of them is lamella blocks already existing in as-spun fibers, and another is the crystallites formed by orientation-induced crystallization during

Table IV Crystallinity (X), Crystallte Sizes (D_{200}, D_{002}, and D_{0140}) of Each Step Fiber

Step	X (%)	D_{200}	D_{002} (Å)	D_{0140}
VD-1	57.6	42.5	42.7	50.2
VD-2	59.1	44.8	43.6	46.8
ZA	58.8	46.1	45.0	52.0

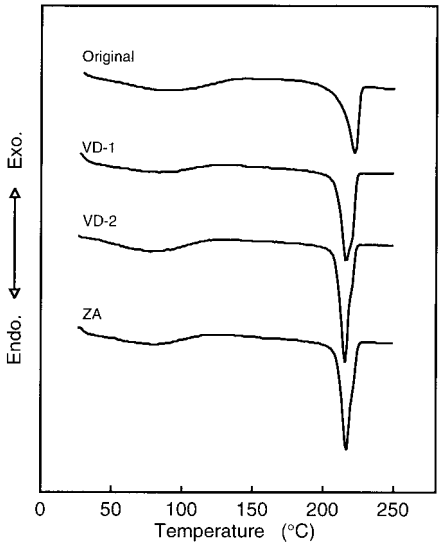

Figure 4 DSC curves for the original, VD-1, VD-2, and ZA fibers.

drawing. If possible, it is desirable that the lamellae are fully soft or/and disintegrated on drawing. So it is necessary that the drawing temperature is as high as possible in the range of nonslippage of molecular chains. The drawing temperature of 190°C was selected after many preliminary experiments. It is much higher than those of the zone drawing (80°C),[1,6,7] the drawing of the salted fiber by Ward et al. (135°C),[4] and the plasticized and gelatinized films by Porter et al. (55–70 and 150°C).[2,9,10] However, it is lower than those for the plugs made of powder crystallized in butanediol by Porter et al. (200°C)[5] and the high molecular weight fiber prepared by dry spinning by Pennings et al. (234°C).[8] However, the limit of drawing temperature for the fiber used by us is 210°C.[17] The discrepancy may be caused by the lower crystallinity and lower molecular weight.

The vibrating drawing process in the present study carried out not only at such a high drawing temperature but also under a suitable vibration and a high stress. The VD-2 performed under a much higher stress of 23 kg/mm^2 than those of the high-temperature zone drawing[17] (13 kg/mm^2) and the multistep zone drawing/zone annealing[7] (18 kg/mm^2).

Change in Superstructure with Processing

Figure 3 and Table III show wide-angle X-ray diffraction photographs, and DR, Δ_t, and f_c and f_a for each step fiber. The DR of 5.5 was easily reached by only at one time of the vibrating hot drawing (VD-1). As the DR is 3.5–4.5 in the case of normal drawing methods except for drawing of the plasticized films[3] or the solution-spun fibers,[8] the value is fairly high. The values of Δ_t and f_a also were all at once reached by the VD-1 up to 63.5×10^{-3} and 0.69, respectively, which are much higher than those of the first-step zone-drawn fibers in the high-temperature zone drawing (53.6×10^{-3} and 0.49) and in the multistep zone drawing (43.8×10^{-3} and 0.51), which are the processes without vibrating. This suggests that the vibrating hot-drawing method is useful to orient the amorphous chains at an earlier stage of drawing. Then the values were stepwise increased with the processing, and finally reached 67.1×10^{-3} and 0.80 of the ZA fiber. The Δ_t value is very high and is higher than the maximum value in the literature (64.5×10^{-3}) attained by the zone-drawing/high-tension annealing method.[12] It corresponds to 86% of the intrinsic crystal birefringence (78×10^{-3}).

Table IV shows the changes in X, and D_{200}, D_{002}, and D_{0140} with the processing. The X was rapidly increased from 27.8% of the original fiber to 57.6% by VD-1, and remained almost constant afterward. The X value is a result of counterbalance between the destruction of lamellae by unfolding and the formation of crystallites by orientation-induced crystallization. As the folded-chain crystals are difficult to be formed on drawing under such a high tension, the increment of X at least can be considered to be the extended-chain crystallites. Compared with the X values of the first-step zone-drawn fibers in the high-temperature zone drawing (41.4%) and in the multistep zone drawing (46%), the value of the VD-1 fiber (57.6%) is strikingly high. It suggests that the crystallization of oriented amorphous chains after unfolding of lamellae took effectively place during drawing. The lateral sizes (D_{200} and D_{002}) increased slightly with the processing, but the

Table V Melting Point and Heat of Fusion for Each Step Fiber

Step	Melting Point (°C)	Heat of Fusion (cal/g)
Original	220.8	10.2
VD-1	217.3	19.7
VD-2	215.8	20.8
ZA	216.9	20.8

Table VI Tensile Properties for Each Step Fiber

Step	Young's Modulus (GPa)	Tensile Strength (GPa)	Elongation at Break (%)
VD-1	14.0	0.53	6.5
VD-2	19.8	0.64	4.9
ZA	23.0	0.80	4.3

length (D_{0140}) decreased by VD-2 and then again increased by ZA.

Figure 4 shows the DSC curves for each step fiber. The endothermic peak became sharper with the processing. The peak for the ZA fiber, however, is fairly broader than those of the high modulus fibers obtained by us.[12] This means that the crystallites have wider distributions in order and/or size.

Table V indicates the melting point and ΔH_f for each step fiber. The former and latter are related to the quality and quantity of crystallites, respectively. The ΔH_f increased with the processing in a similar manner to the X obtained from density. The crystallinities calculated by using the crystal enthalpy of 40 cal/g are 25.5, 49.2, 52.0, and 52.0%, respectively. They are lower by ca. 7% than the X shown in Table IV.

Mechanical Properties

Table VI shows the tensile properties for each step fiber. Young's modulus increased suddenly by only one time of the vibrating hot drawing and reached 14 GPa, as well as DR, Δ_t, f_c, f_a, and X. The modulus and tensile strength were further steeply increased with the following processes, despite the slight increases in DR, Δ_t, f_c, and f_a. The high modulus of 23 GPa for the ZA fiber is higher than that (21 GPa) obtained by the zone drawing/heat treatment under an extremely high tension.[12] The tensile strength, however, is fairly low. The reason comes presumably from the defect of crystalline regions.

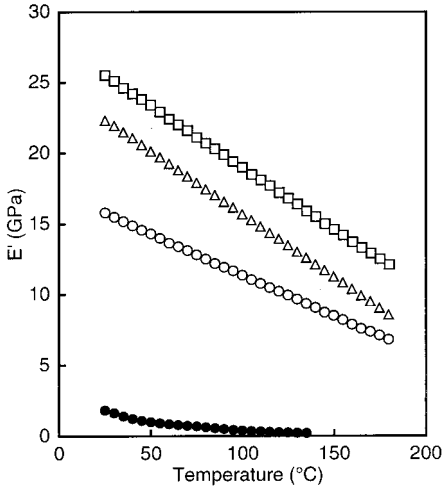

Figure 5 Temperature dependence of dynamic storage modulus, E'; original (●), VD-1 (○), VD-2 (△), and ZA (□).

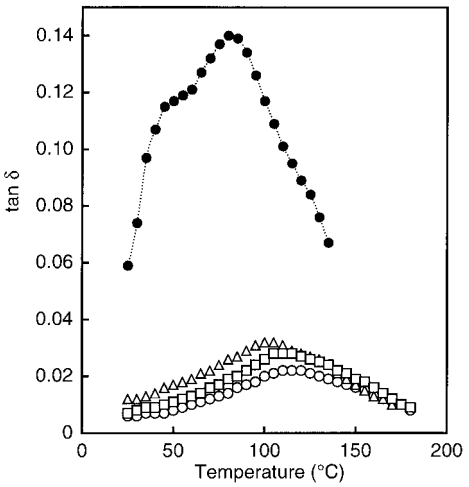

Figure 6 Temperature dependence of tan δ; original (●), VD-1 (○), VD-2 (△), and ZA (□).

Figure 5 show the temperature dependences of dynamic storage modulus (E') for the original, VD-1, VD-2, and ZA fibers. The E' at room temperature increased rapidly in the order of 16, 22.2, and 25.3 GPa with the processing. The E' of 25.3 GPa is the highest value in the literature, which corresponds to 15.3% of the crystal modulus along to molecular chains. The E' decreased almost straight with increasing temperature; the coefficients of correlation for three lines are almost unity. The distinct drop in E' in the temperature range of the α dispersion cannot be seen in Figure 5. Further, the E' retains at a high level at elevated temperatures, for example, 6.7, 8.4, and 12.2 GPa at 180°C for VD-1, VD-2, and ZA fibers, respectively.

Figure 6 shows the temperature dependences of tan δ for the original, VD-1, VD-2, and ZA fibers. The α dispersion peak shifts to a higher temperature and decreases in intensity in the above order. The peak temperature for the ZA fiber (117°C) is very high, and is comparable with that of the multistep zone-drawn/zone-annealed fiber.[7] Further, the peak intensity for the ZA fiber is strik-

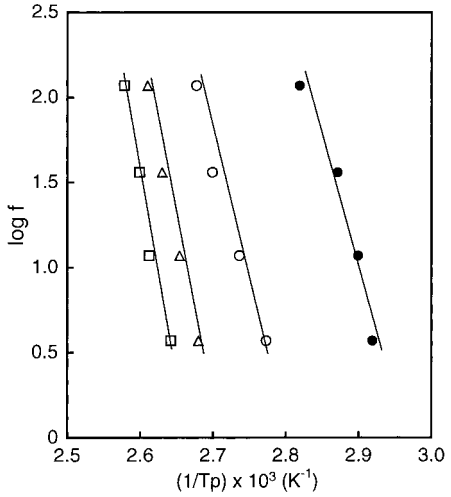

Figure 7 Relation between the logarithm of frequency ($\ln f$) and the reciprocal of peak temperature ($1/T_p$) for α dispersion; original (●), VD-1 (○), VD-2 (△), and ZA (□).

ingly low (0.0225). Compared with 0.27 of 2% LiCl fiber reported by Ward et al.,[4] the intensity is $\frac{1}{12}$. This results in the absence of a distinct drop of E' in the temperature range of the α dispersion. The low intensity and high temperature of the α dispersion peak exhibit that the movements of amorphous chains are small and difficult even in the α dispersion range.

Figure 7 shows the relations between the logarithm of frequency ($\ln f$) used on the measurements of dynamic viscoelasticity and the reciprocal of peak temperature ($1/T_p$) for each step fiber. The apparent activation energies (ΔH_a) calculated from the slope of each line are 65.4, 67.4, 75.0, and 117.3 kcal/mol, in the order of the original, VD-1, VD-2, and ZA fibers. The results also supported that the movements of amorphous chains become difficult stepwise with the processing.

We had studied in detail the effects of drawing and heat treatment on the α, β, and γ dispersion peaks of nylon 6 fibers,[22,23] and it was found that the α dispersion peak was most sensitive to the small differences in superstructure among three dispersions. Also, the temperature of α dispersion peak ($T\alpha$) was found to be proportional to the logarithm of apparent crosslinking density of crystallites ($\ln \sigma_c$), where the crystallites were presumed to act as crosslinking points of amorphous chains.[24] The relationship is similar to that of T_g and crosslinking density in crosslinked polymer, being derived by Fox and Loshaek.[25]

Relationship between Superstructure and Mechanical Properties in an Ultimate Drawn State

As described above, the VD-1 results in the large increments in DR, Δ_t, f_c, f_a, and X, and consequently brings about the excellent mechanical properties. This indicates that the cooperation of vibration, heating, and tension is very effective to form a favorable superstructure in the early drawing process. However, the following processes, VD-2 and ZA, did not distinctly increase the structural factors such as DR, Δ_t, f_a, and X. The modulus and tensile strength are, nevertheless, stepwise and rapidly increased with the processing.

Such an interesting phenomenon appeared occasionally in the fibers drawn until an ultimate state and was confirmed in our experiments. In the study on the heating and cooling cycle (0–180°C) under a vibration (110 Hz) for the twice zone-drawn (ZD-2) nylon 6 fiber, the dynamic storage modulus increased from 17 GPa to 21 GPa, in spite of a slight increase of 5% in DR, whereas Δ_t and X had almost no change. Also, in the study on the process that consists of ZD and annealing under extremely high tension, the E', Young's modulus and tensile strength were remarkably increased from 12, 9.8, and 0.94 GPa of the ZD-2 fiber to 21, 17, and 1.1 GPa of the three-time high-tension annealed fiber, respectively, in spite of slight increases of 0.9 in DR, 4×10^{-3} in Δ_t and 0.066 in f_a, and no change in X and f_c. In both cases, it is clear that the molecular orientation state in the highly drawn fibers cannot be represented by above superstructural factors. It suggests that the molecular chains are oriented, stretched, and strained in molecular level. It is very interesting that the temperature and intensity of α dispersion peak can clearly distinguish the fine difference in the status of amorphous chains. As the amorphous chains are stretched and strained, the peak shifts to higher temperatures and decreases in height in the tan δ–temperature curves.

CONCLUSION

1. The vibrating hot-drawing method was successfully applied to nylon 6 fiber and gave a high dynamic storage modulus at room temperature of 25.3 GPa.
2. The modulus of the ZA fiber remains at a high

level even at elevated temperatures, namely 19 GPa at 100°C and 12.2 GPa at 180°C.
3. In spite of the relatively low draw ratio of 6.0, the high birefringence of 0.067 and orientation factor of amorphous chains of 0.80 were obtained.
4. From the high peak temperature of 117°C and the low peak intensity of 0.0225 of the α_a dispersion peak for the obtained fiber, it was found that the movements of amorphous chains are strongly inhibited.

The authors thank Toray Co. Ltd. for supplying of the original nylon 6 fibers. They also acknowledge the financial supports by the grant-in-aid for the Scientific Research of the Ministry of Education, Science, and Culture, Japan, and by the Eno Kagaku Shinko Zaidan.

REFERENCES

1. T. Kunugi, A. Suzuki, I. Akiyama, and M. Hashimoto, *Polym. Prepr., Am. Chem. Soc. Div. Polym. Chem.,* **20,** 778 (1979).
2. D. Acierno, F. P. La Mantia, G. Polizzotti, and A. Ciferri, *J. Polym. Sci., Polym. Phys.,* **17,** 1903 (1979).
3. A. E. Zachariades and R. S. Porter, *J. Appl. Polym. Sci.,* **24,** 1371 (1979).
4. A. Richardson and I. M. Ward, *J. Polym. Sci., Polym. Phys.,* **19,** 1549 (1981).
5. T. Shimada and R. S. Porter, *Polymer,* **22,** 1124 (1981).
6. T. Kunugi, I. Akiyama, and M. Hashimoto, *Polymer,* **23,** 1193 (1982); **23,** 1199 (1982).
7. T. Kunugi, T. Ikuta, M. Hashimoo, and K. Matsuzaki, *Polymer,* **23,** 1983 (1982).
8. S. Gogolewski and A. J. Pennings, *Polymer,* **26,** 1394 (1985).
9. H. H. Chuah and R. S. Porter, *Polymer,* **27,** 241 (1986).
10. H. H. Chuah and R. S. Porter, *Polymer,* **27,** 1022 (1986).
11. T. Kunugi, A. Suzuki, and K. Chida, *J. Polym. Sci., Polym. Phys.,* **31,** 803 (1993).
12. A. Suzuki, T. Kunugi, and M. Kondo, *Kobunshi Ronbunshu,* **50,** 93 (1993).
13. I. Sakurada and K. Kaji, *J. Polym. Sci., Part C,* **31,** 57 (1970).
14. T. Kunugi and A. Suzuki, *J. Appl. Polym. Sci.,* **62,** 713 (1996).
15. T. Kunugi, H. Ishibashi, and A. Suzuki, *Sen-i Gakkai Prepr.,* F-16 (1991).
16. A. Suzuki, K. Aihara, and T. Kunugi, *Kobunshi Ronbunshu,* **50,** 583 (1993).
17. T. Kunugi, A. Suzuki, and M. Kubota, *Kobunshi Ronbunshu,* **49,** 161 (1992).
18. M. Hashimoto, T. Kunugi, N. Otagiri, and K. Amemiya, *Nippon Kagaku-Kaishi,* **1972,** 454 (1972).
19. T. Kunugi, S. Yokokura, and M. Hashimoto, *Nippon Kagaku Kaishi,* **1976,** 278 (1976).
20. T. Kunugi, M. Moriyama, Y. Yamamoto, and M. Hashimoto, *Nippon Kagaku Kaishi,* **1975,** 1593 (1975).
21. T. Kunugi, Y. Isobe, K. Kimura, Y. Asanuma, and M. Hashimoto, *J. Appl. Polym. Sci.,* **24,** 923 (1979).
22. T. Kunugi, H. Iwasaki, and M. Hashimoto, *Nippon Kagaku Kaishi,* **1981,** 578 (1981).
23. M. Hashimoto and T. Kunugi, *Kogyo Kagaku Kaishi,* **73,** 1501 (1970).
24. T. Kunugi, K. Amemiya, and M. Hashimoto, *Nippon Kagaku Kaishi,* **1973,** 1010 (1973).
25. T. G. Fox and S. Loshaek, *J. Polym. Sci.,* **15,** 371 (1955).